World Academy of Science, Engineering and Technology
International Journal of Structural and Construction Engineering
Vol:17, No:1, 2023

Generative Design of Acoustical Diffuser and Absorber Elements Using Large-Scale Additive Manufacturing

S. Aziz, B. Alexander, C. Gengnagel, S. Weinzierl

***Abstract*—**This paper explores a generative design, simulation, and optimization workflow for the integration of acoustical diffuser and/or absorber geometry with embedded coupled Helmholtz-resonators for full scale 3D printed building components. Large-scale additive manufacturing in conjunction with algorithmic CAD design tools enables a vast amount of control when creating geometry. This is advantageous regarding the increasing demands of comfort standards for indoor spaces and the use of more resourceful and sustainable construction methods and materials. The presented methodology highlights these new technological advancements and offers a multimodal and integrative design solution with the potential for an immediate application in the AEC-Industry. In principle, the methodology can be applied to a wide range of structural elements that can be manufactured by additive manufacturing processes. The current paper focuses on a case study of an application for a biaxial load-bearing beam grillage made of reinforced concrete, which allows for a variety of applications through the combination of additive prefabricated semi-finished parts and in-situ concrete supplementation. The semi-prefabricated parts or formwork bodies form the basic framework of the supporting structure and at the same time have acoustic absorption and diffusion properties that are precisely acoustically programmed for the space underneath the structure. To this end, a hybrid validation strategy is being explored using a digital and cross-platform simulation environment, verified with physical prototyping. The iterative workflow starts with the generation of a parametric design model for the acoustical geometry using the algorithmic visual scripting editor Grasshopper3D inside the Building Information Modeling (BIM) software Revit. Various geometric attributes (i.e., bottleneck and cavity dimensions) of the resonator are parameterized and fed to a numerical optimization algorithm which can modify the geometry with the goal of increasing absorption at resonance and increasing the bandwidth of the effective absorption range. Using Rhino.Inside and LiveLink for Revit the generative model was imported directly into the Multiphysics simulation environment COMSOL. The geometry was further modified and prepared for simulation in a semi-automated process. The incident and scattered pressure fields were simulated from which the surface normal absorption coefficients were calculated. This reciprocal process was repeated to further optimize the geometric parameters. Subsequently the numerical models were compared to a set of 3D concrete printed physical twin models which were tested in a .25 m x .25 m impedance tube. The empirical results served to improve the starting parameter settings of the initial numerical model. The geometry resulting from the numerical optimization was finally returned to grasshopper for further implementation in an interdisciplinary study.

***Keywords*—**Acoustical design, additive manufacturing, computational design, multimodal optimization.

Saqib Aziz is with Berlin University of the Arts, Germany (e-mail: s.aziz@udk-berlin.de).

I. Introduction

THE alarming exponential growth of the global population results in the demand to at least double the available global building stock by 2050. Alongside this, the urbanization of conurbations is leading to an increasing shortage of living and working space. At the same time social demands regarding higher quality of living and comfort standards and the need to build more sustainable and environmentally friendly offer great challenges which the current and future generation must collectively face. When looking at the construction industry, one could argue that only a few significant leaps have been made since the dawn of the modern movement emerging in the first half of the 20th century. Reinforced concrete, a hybrid composite material made of concrete and reinforcing steel is decidedly the leading construction type used around the world as both concrete production accounts for nearly 19% and iron/steel production equates to 25% of the global caused CO_2 emission in the industrial sector [1]. Conventional reinforced concrete flat slab constructions are considered a very economical and adaptable solution. This assessment neglects the enormous material consumption of this construction method, the poor ratio of dead weight and load-bearing capacity, as well as its weaknesses in terms of room acoustics. New technological advancement such as large-scale additive manufacturing could improve and augment such prevailing construction methods. Currently however, there are few research projects [2], [3] that have been able to exploit the high potential of large-format 3D printing with concrete (3DCP) for new application-oriented solutions for a resource-efficient and material-saving construction of reinforced floor structures. The research center TRR 277 “Additive Manufacturing in Construction (AMC) - The Challenge of Large Scale” at the TU Braunschweig for example, explores alternative additive manufacturing processes with concrete (shotcrete 3D printing) in combination with an integrative reinforcement [2]. Another practical application example is the Seehof Castle studio in Lunz, which was designed by the Institute for Structural Design (ITE) at the Technical University of Graz [3], and investigates prefabricated formwork pieces which, when assembled, generate a waffle slab structure. Current research still lacks the ability to take advantage of the potential for developing multi-performative ceiling construction as mono-material systems with integrated building physics functions. The possibilities of

precise material disposition with concrete through 3D printing processes combined with advancements in computer-aided simulation methods and additive processes offer a great potential for new construction methods with a significant reduction in the use of materials with the same or even improved load-bearing capacity, integrated sound absorption, sound insulation and thermal component activation. Research indicates that decision-making process in planning decreases exponentially over time towards the later design development stages [4]. Subsequently, another investigation promotes that performative design optimization processes in the early planning stages can have significant benefits for the economic and ecological performance of the building [5]. Therefore, a transdisciplinary design and decision-making process allowing designers and engineers to foster their design exploration with numerical data would be advantageous and necessary.

Ultimately, a more intelligent planning of the building physics would be most beneficial to the occupants of a building. As research shows we spend about 87% of our time indoors [6] and an inefficient planning of the indoor microclimate leads to non-negligible negative health issues. The Sick Building Syndrome (SBS), for example, is a building related illness occurring primarily in office, medical and educational facilities, which describes physical and psychological health deficiencies and negative effects on the perceived well-being [7]. Most notable factors causing the SBS are related to fluctuating temperatures and humidity levels and/or disturbing noise pollution, resulting in negative impact on the health and work productivity [8]. To prevent this, mechanical systems are usually used, which are associated with high operating costs and their own losses in comfort. Thermally Activated Building Systems (TABS) can be very effective in conditioning the indoor microclimate [9]. Here, a fluid is pumped through an integrated duct network, mostly located in ceilings and/or walls to cool or heat the space. The effectiveness of such TABS systems is largely dependent on direct energy exchange with the interior space and any type of shading, such as retrofitted acoustic ceilings, has a relatively high negative performance impact [10]. Currently only a limited offering of hybrid systems/solutions enabling integrated room thermal and acoustical performance can be found on the market [11], while none that utilizes additive manufacturing to create a mechanical, thermal, and acoustical integrated and mono-material system.

II. Background

A brief review of the development of Helmholtz resonator based acoustic absorber materials and structures in the last decade will show that there are a plethora of calculation and design methods for finding geometries which provide tunable sound absorption in a specific frequency range or even perfect absorption at a target frequency. For example, in 2021, Mahesh et al. [12] developed a numerically validated deep neural networking scheme for the inverse design of a compound Helmholtz resonator and microperforated panel structure. A highly effective split-tube resonator structure, characterized as an acoustic metamaterial, maintaining a sub-wavelength module thickness was developed and validated using the finite element method by Wu et al. in 2016 [13]. Another acoustic metamaterial based on the construction of resonant folded channels provides good absorption at lower octaves and was tested to evaluate thermo-viscous losses in COMSOL Multiphysics [14], as described in a 2019 paper from Wu et al. [15]. Combined numerical, empirical, and analytical studies on resonator neck structures which are geometrically optimized using, for example, embedded spiral neck structures [16], or aeroacoustic design principles [17] show that precise narrowband resonators can be effectively planned for implementation in noise control engineering problems. Even advances have been made in the design and manufacturing of low-frequency sound absorbers whose effective range extends below the conventionally required material thickness for perfect absorption at the same frequency [18]. For nearly half a decade, 3D printing techniques have been utilized for broadband low-frequency damping in the form of decorated membrane absorbers, albeit at a relatively small scale for a mounted device [19]. Characterizing only a small selection of the many methodological and material advances made in acoustic absorber design, one finds that the structures investigated indicate the necessity to manufacture and install an additional material or device into an architectural or technical environment to achieve sufficient damping. The following study outlines the methodology and results of using an interdisciplinary approach to incorporate broadband acoustic damping directly into the primary structure of a building, thus decreasing the reliance on retrofitting and post-construction room acoustic treatments.

By using large-scale three-dimensional concrete printing (3DCP) the novel construction method enables the production of innovative building components such as ceiling slabs and wall elements in a semi-prefabricated construction sequence, whose physical properties (acoustics, thermal and mechanical) can be optimized geometrically and materially by a multimodal computer-aided design and analysis process and subsequently manufactured additively by a specially programmed print path generation. The construction method is limited to two material components: compression-resistant mineral materials such as concrete, which can be processed in additive manufacturing processes, and high-tensile materials such as reinforcing steel or artificial fibers (carbon, glass), which are added manually or automatically. The process allows a material saving of concrete of 45% for point-supported reinforced concrete flat slabs with comparable spans and loads and thus a significant improvement in the balance of the component-related CO_2 balance within the framework of a Life Cycle Assessment (LCA). This is essentially achieved by forming a ribbed or hollow core slab in semi-precast construction, consisting of a uniaxially or biaxially tensioned beam grid and one or two cover slabs. The prefabricated parts of the formwork body (FB) required for production are not made of plastics or metals but of mineral materials such as concrete and are prefabricated in additive manufacturing processes. The decisive factor here is the possibility of manufacturing many highly customizable geometrically optimized elements in the preceding computer-

aided design and planning process, which together result in a high multimodal performance of the component (ceiling, wall) in its spatial disposition. The additively prefabricated FB are arranged on a falsework scaffold at the installation site as permanent formwork, creating near-zero waste and are completed with in-situ concrete after adding reinforcement.

III. Methodology: Acoustic Absorber Formwork

The integrative and multipurpose formwork function as acoustic absorber and diffuser elements which, as individual elements or as a combined spatial system, can be acoustically calibrated only by means of their detailed geometric definition, to achieve a highly customizable and DIN standard conform (according to the type of use) room acoustical performance. As a result, the equivalent sound absorption areas of rooms are influenced in such a way that all use-dependent necessary acoustic threshold values (absorption, diffusion, reverberation, scattering) can be met. The basic principle is fostered by the implementation of the mechanical properties of Helmholtz resonators in the geometric definition and planning of the additive manufactured formwork elements. For this purpose, a cyclical and iterative process chain was developed for the generation and optimization of the formwork, which essentially consists of four modules: i) Computer-aided creation of the spatially networked basic geometries of the formwork elements in a CAD/BIM modeling software with a visual programming interface such as Rhinoceros and Grasshopper3D [20], ii) Automated generation of the individual formwork with integrated Helmholtz absorber and diffuser properties, iii) Validation and optimization of the formwork geometry by an FEM simulation program such as COMSOL Multiphysics, feedback of the numerical evaluation and optimization of the acoustic properties of the individual elements and the overall system, iv) Generation of the machine or g-code for the robotic fabrication. The individual functions and processes are explained in more detail in the following chapter and subchapters.

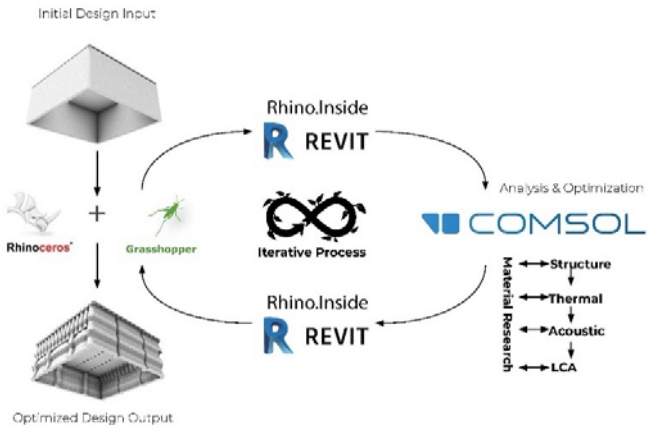

Fig. 1 Visualization of the multi-objective optimization process

A. Definition of the Initial Geometry

The definition of the topological properties of the FB such as height, width, and length result from the consideration of the global load bearing and serviceability of the ceiling and/or wall construction system, building physics criteria and design factors. From a design point of view, e.g., the alignment lines of a façade and/or the room layout can be considered in the placement and design of the FB. To further specify the definition of the FB and its integrated acoustic zones (Fig. 5), an initial room acoustic validation follows, using ray tracing algorithms. Here, further geometric specifications of the room-related absorption ranges to be achieved (broadband frequency ranges between 100 Hz and 1000 Hz) and geometric considerations of surface orientation regarding the room mode shape are addressed, though room modes are simulated using FEM. From these evaluations, the geometries of the horizontal guide curves of the FB are derived and vertically extruded. The height can be variably adapted to the necessary structural parameters. The variation of the basic bodies of the FB helps to increase the diffusivity of the sound field in the frequency range of the high centers. On a smaller scale, the surface roughness/ texturing created in the printing process is suitable for diffuse reflection of high frequencies and thereby preventing the generation of flutter echoes, for example. The following special features are possible:

- The extrusion can be formed in a straight line but also created in more spatially complex manner.
- The upper level of the extrusion is usually planar but can also vary in height.
- The total height of the extrusion is usually 100 mm to 350 mm (Fig. 2).
- The design as a closed hollow body is also possible (Fig. 3).

Depending on the application and the technical equipment of the additive manufacturing cell (robot arm, gantry system), the extrusions are divided into smaller and vertically successive printing levels using a process called slicing. The minimum and maximum height of the printing planes depends on the technical equipment and ranges between 3 mm to 10 mm. In principle, continuous as well as discontinuous print paths can be implemented. For the formation of the absorber and diffuser geometries of the FB, the created print layers are vertically combined into zones (Fig. 5): Ceiled Zone, Absorber Zone and Diffuser Zone. Another zone - the Filling Zone - describes the entire volume that is poured with fresh concrete on the construction site. The respective height of the absorber zone is parameterized and automatically derived from the preceding acoustic validation. Manual setting for design reasons is also possible. After the zoning of the individual formwork, the final geometry definition of the FB takes place.

B. Algorithmic and Semi-Automated Geometry Generation

Based on the information regarding the height of the absorber zone, a geometric approximation of optimal Helmholtz absorber geometries as cavities is automatically generated into the basic structure of the FB. The algorithm is developed to determine resonance frequencies for Helmholtz resonators and is implemented in the computer-aided planning and manufacturing tool of the FB. The algorithm can vary the parametrically variable geometric properties (resonator neck in

length and diameter, number of resonator necks and resonator volume) of the resonator to change the amount of absorption at resonance and increase the bandwidth of the effective absorption range. This method allows a FB to absorb different and/or broadband frequency bands by coupling a varying number and geometry of air volumes in combination with a varying number and geometry of neck volumes. The spatial network of differently and/or similarly tuned acoustic absorbers FB offers a high degree of freedom when dealing with large architectural spaces and enables different acoustic measures for varying room areas or usage profiles while using a consistent process chain. The definition of the three zones of the FB is automated in real time and the exact processes of geometry generation can be summarized as follows:

1) The first 2 to 3 print levels - approximately 20 mm (varying according to size) are used to form a load-bearing bottom of the FB (ceiled zone). The path can be polygonal, spiral, radial, serpentine or meandering (Fig. 4). In addition, to prevent holes or the formation of joint gaps in the bottom of the FB, the distances between the individual adjacent print lanes below and above are calculated iteratively and the dimensions of the print lanes are adjusted accordingly.
2) The formation of this absorber zone with the integrated Helmholtz volumes is done, among other things, by uniaxially or biaxially tapering and meandering print paths. Negative volumes varying in width, height and length can be formed as chambers and different hollow resonator neck geometries. The height of this absorber zone should be at least 50 mm and can be formed up to the total height of the extrusion of the FB. If the entire height is used, the diffuser zone is omitted, and the variation of a hollow FB is created (see Fig. 3).

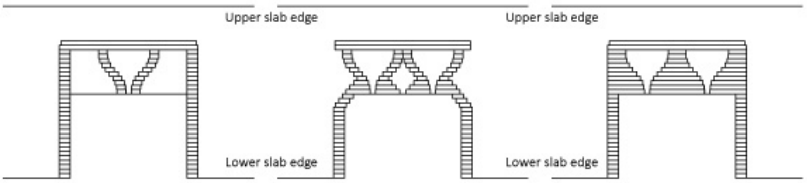

Fig. 2 Formwork variation for a two-way joist slab

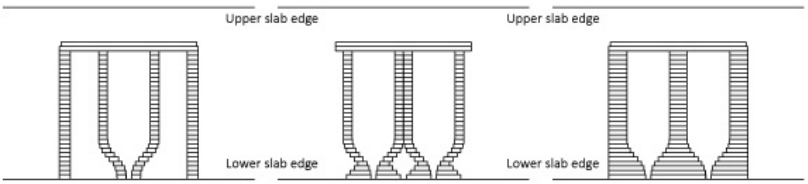

Fig. 3 Formwork variation for a hollow core slab

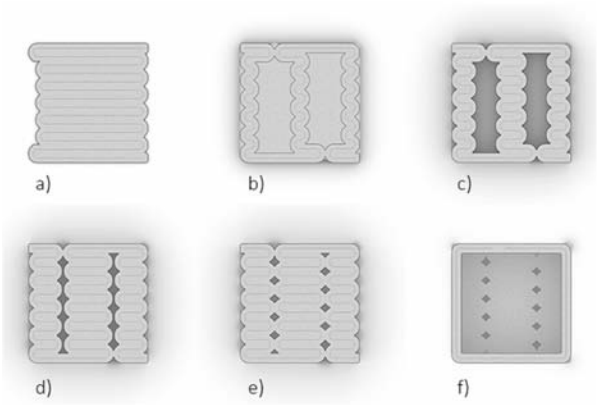

Fig. 4 (a)-(f) visualization vertical print-path evolvement (Top view)

During the formation of the negative space, an algorithm ensures that all distances of the individual adjacent, underlying, and overlying print paths are iteratively calculated and adjusted to guarantee the manufacturability of the overall structure (inspection of overhang distances). The tapering is formed in such a way that, for the selected height of the absorber zone, a closed ceiling results approaching the top, in which only the resonator neck openings are visible as recessed holes. The resonator necks can also be formed as slit geometries.

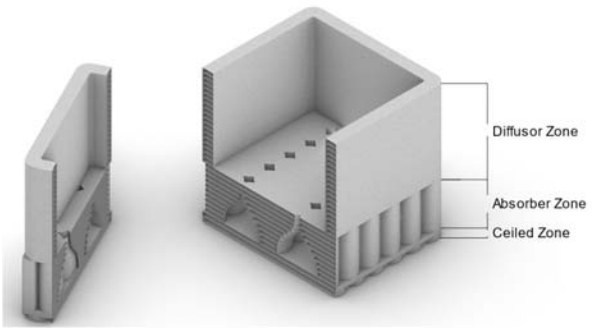

Fig. 5 Visualization of integrated absorber cavities

3) In the upper part of the FB (diffuser zone), a three-dimensional wave structure is implemented with the aim of scattering incident sound waves and reducing the unwanted effect of the otherwise uniformly reflected sound. The diffuser effect is calculated by a mathematical procedure and formed as a geometric wave structure in an automated way, whereby further geometric irregularities and structures can produce similar scattering effects. An algorithm also checks and optimizes the manufacturability

of the structure. Due to the high geometric flexibility in the production of this diffuser zone, the sound waves can be distributed in the room according to both quantitative and qualitative criteria either uniformly or in a targeted manner. The formation of interference effects caused by the superimposition of reflections due to different depressions and patterns can be advantageously integrated.

IV. Methodology: Validation and Optimization of the Integrative Formwork using Finite-Element-Methods

A. Measurement of Absorption Coefficients in Impedance Tube

Strong low frequency absorptive behavior was expected from the printed structure. Since the error of absorption coefficient assessment via methods conducted according to ISO 354:2003 [21] increases at lower octave bands, the impedance tube method was chosen as the more suitable measurement for the purpose of this experiment. An added benefit of obtaining absorption coefficients from the impedance tube measurements is that results may be directly compared with simulation results, given that both sets of absorption coefficients describe sound behavior orthogonal to the absorber surface. The same comparison may not be made with results obtained from reverberation chamber experiments, since the absorption coefficients that were obtained from the conducted measurements are only applicable for diffuse field excitation.

The measurements were conducted in a large, square-sectioned impedance tube at the testing facility of the department of engineering acoustics at the Technical University of Berlin. The dimensions of the tube are 0.25 m in depth and 0.25 m in width, allowing for accurate measurements in the frequency range of 20 Hz to 680 Hz. Class 1 measurement microphones were inserted at heights of z_1 = 1.9 m, z_2 = 2.52 m, and z_3 = 2.75 m. Though the measurement was conducted according to ISO 10534-2:1998 [22] using the transfer function method, which conventionally uses two microphone positions, a third position farther away from the test specimen along with the microphone closest to the probe allow for greater accuracy at lower frequencies where wavelengths begin to approach critical lengths and differences in phase become harder to detect when the microphones are too close together.

Fig. 6 Visualization of the three variations as negative voids

Three concrete probes with varying inner resonator volumes ($V_1 = 8 \times 10^{-5}$ m^3, $V_2 = 1.6 \times 10^{-4}$ m^3, and $V_3 = 4 \times 10^{-4}$ m^3) but constant resonator neck geometries were printed for the measurements. The dimensions along the outer edges were 0.25 m x 0.25 m x 0.25 m, as shown in Fig. 5, providing them a tight fit within the impedance tube. Dense window kit was used to seal the top edges of the probes where the cement meets the adjacent metal wall of the impedance tube to avoid any edge effects which would allow for additional slit-like absorption in the thermal layer during measurements. The specimens were placed directly on the floor of the impedance tube.

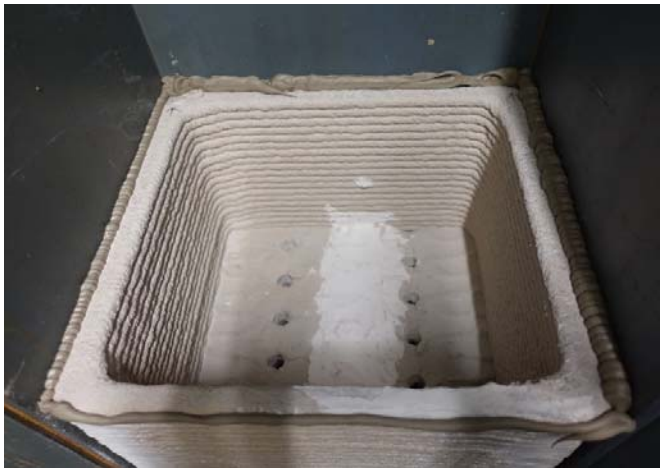

Fig. 7 Physical prototype inside the impedance tube

Various numbers and configurations of resonator neck openings were measured, including 2, 4 (closely spaced), 4 (widely spaced), 6 (closely spaced), 6 (widely spacing), and 10 to test for differences resulting from changes to resonator array geometry. The holes were tightly plugged with a compressible foam, which allowed no air to move through the plugged hole. As described in ISO 10534-2:1998 [22], after calibration and an initial phase correction within the data, the measured pressures were recorded and processed within the test software which outputs the transfer functions of the total, incident, and reflected sound fields necessary to calculate the complex reflection factors with the equation:

$$r = H12 - HIHR - H12e2jk0x1 \quad (1)$$

in which H_{12} represents the transfer function of the total sound field, H_I and H_R the transfer functions of the incident and reflected sound fields, respectively, k_0 the wave number of the frequency in question, and representing the distance between microphone positions. The resulting reflection factor allows for the simple calculation of the absorption coefficient following the equation

$$\alpha = 1 - |r|2. \quad (2)$$

B. Development of a Numerical Model

Analog to the impedance tube experiments, the implementation of a well-tested and validated numerical modeling technique using the finite element method was used to conduct simulations of incident and reflected sound fields orthogonal to the surface of the printed concrete structure. The discretized geometry, representing the negative space from the physical structure of the actual printed slab, as seen in Fig. 8, was created in Grasshopper and imported into COMSOL Multiphysics via Rhino.Inside [23] and LiveLink for Revit [24].

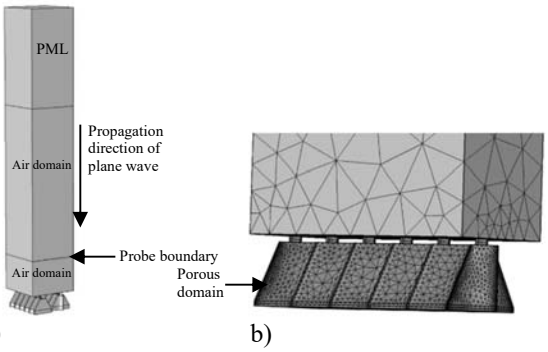

Fig. 8 (a) Numerical model; (b) Detail of meshed resonator volume

The simulation principle was to develop a virtual impedance tube in which plane waves, defined as a background pressure field, with an amplitude of A = 1 Pa were sent orthogonally towards the resonator structure openings and reflected into the tube from which they could exit with perfect attenuation using perfectly matched layers (PML). At a height z = 0.15 m above the resonator surface, incident and reflected pressure fields were probed and averaged over the entire surface parallel to the structure. The complex reflection factor was calculated with,

$$r_{\text{sim}} = \frac{p_{\text{scat}}}{p_{\text{inc}}} \tag{3}$$

from which the absorption coefficients could be calculated analog to (2) with $\alpha_{\text{sim}} = 1 - |r_{\text{sim}}|^2$.

Highly resonant numerical acoustic models in which all external boundaries are considered to be sound hard benefit from the addition of slight damping to increase accuracy in the results. For this reason, a porous domain was included within the resonator cavity with a minimal fluid resistance of 50 Pa·s·m^{-2}.

C. Shape Optimization of Numerical Model

An objective of the printed concrete structure is to not only provide sufficient base damping in a single frequency band, rather in a broadband manner by generating a constellation of various resonator proportions and geometries. In order to find a set of physically realizable resonator geometries with resonant frequencies ranging from 125 Hz to 630 Hz, a general shape optimization study step was conducted within the FEM software. A set of reference absorption coefficient values, defined as Gaussian pulse functions were provided to the model. The referred to equation was as follows:

$$\alpha\text{obj}(f) = a \cdot e^{-(f-b)22c2} \tag{4}$$

In this equation, a has a maximum magnitude of 1, f and b are frequency and function shift coefficients, and c a scaling factor, an objective expression. These values were derived by using the following equation:

$$X = \sum(\alpha_{\text{obj}}^2 - \alpha_{\text{sim}}^2) \tag{5}$$

In this equation X represents the difference of the squared reference function and the squared simulated absorption coefficients summed over all frequencies and could be minimized using a Bound Optimization by Quadratic Approximation (BOBYQA) method. A gradient free method such as this is especially suited for this type of problem, where the fitting of parameters redefining the model geometry need to contain both discrete integer steps, such as number of resonator necks, as well as scaled adaptation steps in the millimeter range, for example in resonator neck width radius. In addition, the BOBYQA minimization method effectively finds local minima of non-linear function sets in multi-parameter tasks. Four control variables, or parameters, were used to evaluate the optimized geometry for the intended resonant frequency including resonator cavity depth controlled by the domain extrusion height, resonator neck height, resonator neck radius, and number of resonator necks. Since the optimization algorithm must evaluate parameter values between whole numbers, a dummy variable was defined to round the evaluation step to the nearest whole number to allow for a discrete value controlling the number resonator necks within the resonator neck array geometry node. The completed simulation returned the optimized geometry as well as the numerical values of the control parameters, which could be fed back into the generative model in Grasshopper respectively via LiveLink for Revit.

V. Methodology: Feedback FEM to CAD

After the FEM optimization process (Section III), the modified geometric variables are fed back into the CAD/BIM software e.g., Rhinoceros/Grasshopper3D in real time. The geometry generating variables are reinstated by the optimized values deceived form the FEM optimization and form the basis of the acoustically optimized final geometry of the FB. This process can be repeated iteratively to make further mechanical, acoustical and aesthetic adjustments or to generate design variants. After the completion of the iterative design and optimization process a custom algorithm can automatically generate the source code or machine code needed for the additive manufacturing process to produce the final physical artefact fostered by the numerical result. In this process step, further manufacturing parameters such as the printing speed, the printing volume, the material-dependent plastic characteristics of the printing mixture and the technical capacities of the respective robotic manufacturing station can be integrated into the generative manufacturing process of the FB allowing further variations in finishes and resolution quality.

Fig. 9 Images of the printing process

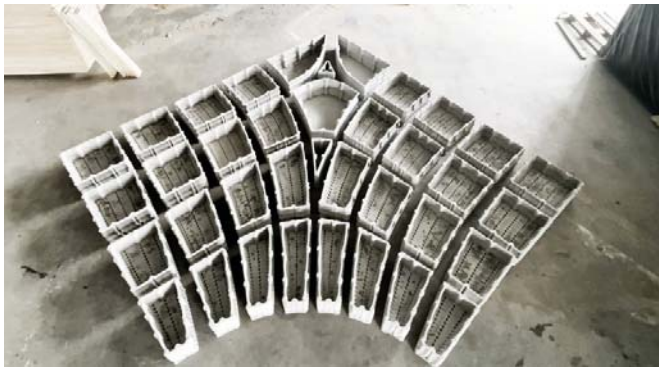

Fig. 10 Image of physical mockup

VI. Results

The impedance tube measurements tested for shifts in frequency and magnitude of absorption peaks of resonant frequencies in the structure as a result of variable resonator cavity volumes and number of resonator necks while it is mathematically evident that a larger resonator cavity decreases the resonant frequency f_{res} (in Hz), according to:

$$f_{\text{res}} = \frac{c_0}{2\pi}\sqrt{\frac{S_{\text{neck}}}{V_{\text{cavity}} l_{\text{neck}}}} \tag{6}$$

where c_0 is the speed of sound, S_{neck} the surface area of the resonator neck, V_{cavuty} the volume of the resonator cavity, and l_{neck} the length of the resonator neck. It could be observed that an increase or decrease in open resonator necks within an array as compared to the control specimen resulted in a highly discernible shift in the resonant frequency of the printed resonator structure. Fig. 11 shows the absorption coefficients of all probes measured in the impedance tube, the properties of which are listed in Table I.

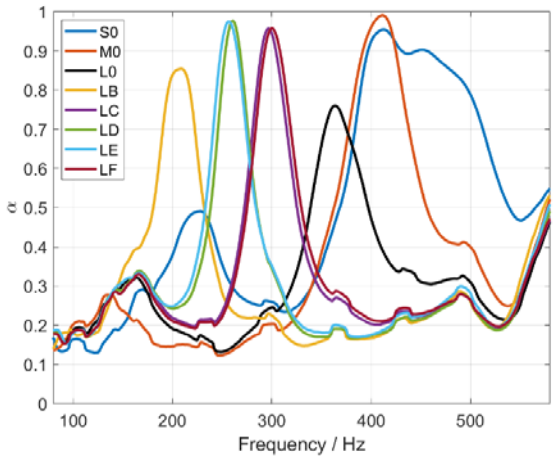

Fig. 11 Results of impedance tube measurements

As the results show, while increases to the cavity volume lower the resonant frequency, an additional reduction of resonator neck openings further decreases the resonant frequency for the same resonator cavity volume. Changes to hole spacing seem to have a minimal effect on the resonant frequency and the magnitude of its absorption.

TABLE I
Properties of Test Probes

Probe	Volume in m^3	Number of open resonator necks
S0	8×10^{-5}	10
M0	1.6×10^{-4}	10
L0	4×10^{-4}	10
LB	4×10^{-4}	2
LC	4×10^{-4}	6 widely spaced
LD	4×10^{-4}	4 widely spaced
LE	4×10^{-4}	4 closely spaced
LF	4×10^{-4}	6 closely spaced
S0	8×10^{-5}	10
M0	1.6×10^{-4}	10
L0	4×10^{-4}	10

Initial FEM simulations of a detailed model, which was based on the same geometry as the probe L0, whose resonant frequency lies at f_{res} = 364 Hz and an absorption of α_{res} = 0.76, returned absorption coefficients with a resonant frequency of f_{res} = 340 Hz with α_{res} = 0.75. The results of the geometry optimization procedure, as seen in Fig. 12, show that automated changes to the above-described geometric parameters will indeed achieve broadband absorption below 800 Hz, with maximum absorption ranging between 0.50 and 0.70.

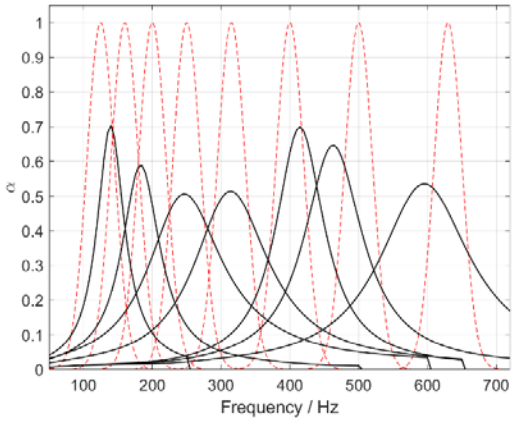

Fig. 12 Results of FEM simulation (solid black: simulated absorption coefficient; dashed red: reference functions)

VII. Conclusion

As the empirical measurements show, a generative design process and workflow for the manufacturing of a 3D printed acoustic absorber structure based on Helmholtz resonator array geometries can successfully be integrated into early building planning phases and reduce the later need to add redundant acoustic absorber materials. The structure described can provide a significant level of broadband base damping for frequencies as low as 125 Hz with 70% absorption. As design conflicts arise between acoustic engineers, architects, and other consulting engineers regarding the technical and aesthetic functions of inner building surfaces, planning expenses can rise while the room acoustic quality of the end result may decrease due to compromises made by the acoustic engineer. This often

leads to the requirement of additional absorber materials installed after the fact by tenants, which may or may not compete with other physical aspects of the architecture, be they visual or technical. Additionally, stringent spatial requirements placed on planning acousticians increase the difficulty in meeting various requirements for room acoustic comfort in workplaces, for example those stated in norms such as the DIN 18041:2016-03 [25], 24. ASR A 3.7:2021-03-24 [26], and VDI 2569:2019-10 [27].

The presented work aims to foster the collaboration between an interdisciplinary group of designers and engineers and offers a methodology that could significantly benefit the early-stage design as well as the following project related decision-making processes and allows to conceptualize and prototype entirely novel and innovative building structures only conceivable by a highly active interdisciplinary collaborative effort and state of the art technological advancements. By incorporating not only a broadband effective acoustic design solution into the planning of the primary structure, combined with the advantage of macro and micro level geometric articulation of the design, while also being capable of including other mechanical, thermal but also aesthetic requirements, a more efficient execution of the building structure can be achieved, resulting in spaces with a higher degree of user comfort for a plethora of parameters. Future studies could involve a FEM-based and empirical assessment of the sound reduction index of such a large-scale printed structure, as well as utilizing a FEM model for predicting acoustic scattering coefficients. Additionally, researching and defining a set of design algorithms which incorporate Multiphysics simulations of thermal and static properties of the structure conducted alongside acoustic design optimization schemes would ultimately provide an ideal foundation for an adaptable and efficient solution for solving multiple building physics problems in an integrative way.

ACKNOWLEDGMENT

This research and particularly the additive manufacturing process and prototyping were supported by the Department for Structural Design (ITE) led by Prof. Stefan Peters at the Technical University of Graz. We would like to especially thank Robert Schmid, Georg Hansemann, and Christoph Holzinger. We thank our colleague Max Weber from the structural engineering office Bollinger + Grohmann Ingenieure located in Berlin, Germany who provided insight and expertise that greatly assisted the research. The work of Bradley Alexander is funded by the Stiftung Casa Acustica in Berlin.

REFERENCES

[1] J. Allwood, J. Cullen, “Steel, aluminium and carbon: alternative strategies for meeting the 2050 carbon emission targets”, 2009.
[2] H. Kloft, M. Empelmann, N. Hack, E. Herrmann and D. Lowke, “Reinforcement Strategies for 3D-Concrete-Printing”. *Civil Engineering Design*, 2.10.1002/cend.202000022, 2020.
[3] G. Hansemann, R. Schmid, C. Holzinger, JP. Tapley, HH. Kim, V. Sliskovic, B. Freytag, A. Trummer and S. Peters, “Additive Fabrication of Concrete Elements by Robots: Lightweight concrete ceiling”. *in Fabricate 2020: Making Resilient Architecture,* UCL PRESS, London, S. 124-129, 2020.
[4] N. Kohler and S. Moffatt, “Life-Cycle Analysis of the Built Environment”, *United Nations Environment Programme Division of Technology*, Industry and Economics Publication, UNEP Industry and Environment, 2003.
[5] H. Gervásio, P. Santos, R. Martins and L. S. da Silva, “A macro-component approach for the assessment of building sustainability in early stages of design”. *Building and Environment*, 73, 256-270, 2014.
[6] NE. Klepeis, WC. Nelson, WR. Ott, JP. Robinson, AM. Tsang, P. Switzer, JV. Behar, SC. Hern and WH. Engelmann, “The National Human Activity Pattern Survey (NHAPS): a resource for assessing exposure to environmental pollutants”, *J Expo Anal Environ Epidemiol*. 2001,
[7] A. Ghaffarianhoseini, H. AlWaer, H. Omrany, A. Ghaffarianhoseini, C. Alalouch, D. C.-C. and J. Tookey, “Sick building syndrome: are we doing enough?”, *Architectural Science Review*, 61:3, 99-121, 2018.
[8] N. Ghodrati, M. Samari, M.W. Mohd Shafiei, “Green Buildings Impacts on Occupants' Health and Productivity”, *Journal of Applied Sciences Research*, 8, 4235-4241, 2012.
[9] B. Lehmann, V. Dorer and M. Koschenz, “Application range of thermally activated building systems tabs”, *Energy and Buildings*, Volume 39, Issue 5, Pages 593-598, ISSN 0378-7788, 2007.
[10] L. Marcos Domínguez, Ongun B. Kazanci, Nils Rage and Bjarne W. Olesen, “Experimental and numerical study of the effects of acoustic sound absorbers on the cooling performance of Thermally Active Building Systems”, *Building and Environment*, Volume 116, Pages 108-120, ISSN 0360-1323, 2017.
[11] Innogration GmbH, 2013, Thermoaktive Fertig-Betondecken für verbesserte Raumakustik, accessed 27 January 2022, <https://www.firmenpresse.de/pressinfo924910/thermoaktive-fertig-betondecken-fuer-verbesserte-raumakustik.html>.
[12] K. Mahesh, S. Kumar Ranjith, and R.S. Mini, “Inverse design of a Helmholtz resonator based low-frequency acoustic absorber using deep neural-network,” *Journal of Applied Physics* 129, 174901, 2021
[13] Xiaoxiao Wu, Caixing Fu, Xin Li, Yan Meng, Yibo Gao, Jingxuan Tian, Li Wang, Yingzhou Huang, Zhiyu Yang, Weijia Wen, et al., “Low-frequency tunable acoustic absorber based on split tube resonators,” *Applied Physics Letters* 109, 043501, 2016
[14] Software Comsol Multiphysics https://www.comsol.com/
[15] Fei Wu, Yong Xiao, Dianlong Yu, Hongang Zhao, Yang Wang, Jihong Wen, et al., “Low-frequency sound absorption of hybrid absorber based on micro-perforated panel and coiled-up channels,” *Applied Physics Letters* 114, 151901, 2019
[16] Jingwen Guo, Xin Zhang, Yi Fang, Ziyan Jiang, “A compact low-frequency sound-absorbing metasurface constructed by resonator with embedded spiral neck,” *Applied Physics Letters* 117, 221902, 2020
[17] F. Caeiro, C. Sovardi, K. Förner, W. Polifke, “Shape Optimization of a Helmholtz resonator using an adjoint method,” *International Journal of Spray and Combustion Dynamics,* vol. 9(4) pp. 394–408, 2017
[18] Y. Aurégan, “Ultra-thin low frequency perfect sound absorber with high ratio of active area,” *Applied Physics Letters* 113, 201904, 2018
[19] A. Leblanc, A. Lavie, “Three-dimensional-printed-type acoustic metamaterial for low frequency sound attenuation,” in *The Journal of the Acoustical Society of America* vol. 141, EL538; doi: 10.1121/1/4984623, 2017
[20] Software Rhino 6 with Addon Grasshopper3D https://www.rhino3d.com
[21] ISO 354:2003 Measurement of sound absorption in a reverberation chamber
[22] DIN EN ISO 10534-2:2001-10. Acoustics - Determination of sound absorption coefficient and impedance in impedance tubes - Part 2: Transfer-function method (ISO 10534-2:1998); German version EN ISO 10534-2:2001
[23] Software Addon Rhino. Inside Revit https://www.rhino3d.com/inside/revit/1.0/.
[24] Software Autodesk Revit https://www.autodesk.com.
[25] DIN 18041:2016-03 Acoustic quality in rooms - Specifications and instructions for the room acoustic design
[26] ASR A 3.7:2021-03-24 Technische Regeln für Arbeitsstätten - Lärm
[27] VDI 2569:2019-10 Sound protection and acoustical design in offices